Supplementary document.

Parabola-like gold nano-bowtie on sapphire substrate as nano-cavity

Wenbing Li[1], Zhuo Yang[1,2], Jiali Zhang[1,2], Xin Tong[1,2], Yuheng Zhang[1,2], Bo Liu[1,2], Chao Ping Chen[3]

1 Shanghai Industrial micro-technology Research Institute, No.235, Chengbei Road, Jiading, Shanghai, China. Quentin.li@sitrigroup.com (W.L.)

2 School of Microelectronics, Shanghai University, No.20, Chengzhong Road, Jiading, Shanghai, China. yz98@shu.edu.cn (Z.Y.); jallyzhang@shu.edu.cn (J.Z.); tongxin@shu.edu.cn (X.T.); 1170832697@shu.edu.cn (Y.Z.)

3 Smart Display Lab, Shanghai Jiao Tong University, No.800, Minhang, Shanghai, China.

Corresponding author:

steven.liu@sitrigroup.com (B.L.)

ccp@sjtu.edu.cn (C.P. C.)

In the Fourier domain, the dispersion of the relative permittivity can be expressed as a function depends on both the wave vector and angular frequency of light [1],

$$\varepsilon(\vec{K},\omega) = 1 + \frac{i\sigma(\vec{K},\omega)}{\varepsilon_0 \omega} \qquad (1)$$

With a limit of spacial local response, it can be simplified as [1],

$$\varepsilon(\vec{K} = 0,\omega) = \varepsilon(\omega) \qquad (2)$$

It becomes the type we normally see, in which the permittivity only depends on the frequency of incident light. The dispersion of the permittivity for gold material follows the Drude model, with an assumption that the electrons in gold material are free without the bounding from nuclei. The modified Drude model with multiple Lorentz terms expressed as [2],

$$\varepsilon(\omega) = \varepsilon_\infty + \frac{\sigma/\varepsilon_0}{j\omega} + \sum_{p=1}^{p} \frac{C_p}{\omega^2 + A_p j\omega + B_p} \qquad (3)$$

As explained by F. Hao, with the parameters given in reference [2] in followed table, the refractive index values obtained from Ciesielski [3] [4] can be fitted with a Drude model with four Lorentz terms.

$\varepsilon_\infty = 1$ $\quad \sigma/\varepsilon_0 = 1355.01$

	$A_p(eV)$	$B_p(eV^2)$	$C_p(eV^3)$
p=1	-8.58E-04	-1.16E+04	5.56E+07
p=2	-2.875	0	2.08E+03
p=3	-997.6	-3090	6.92E+05
p=4	-1.63	-4.409	26.15

The refractive index of sapphire (Al_2O_3) was obtained from reference [5], and it can be fitted with a three-terms Sellmier model [6] with parameters from reference [3].

$$n^2 = 1 + \sum_{p=1}^{3} \frac{B_p \lambda^2}{\lambda^2 - C_p} \qquad (4)$$

The n and k values are also fitted with a multiple coefficients FDTD model, and make the root mean square error (RMS) is less than 0.1 before the simulation. The graphs about the n and k values of gold material and sapphire used in this calculation are displayed in Fig.S1.

The values of the scattering cross section, absorption cross section, and extinction cross section dependent on resonance wavelength with variation of each geometry parameter, and the relationship between various geometry parameters and the resonance wavelength, are displayed in Fig.S2 to Fig.S4 as a supplement.

The absorption ratio depends on resonance wavelength according to the variation of wing width, gap size, and thickness, and also the relationship between the geometry parameters and the resonance wavelength, are displayed in Fig.S5 as a supplement.

The average field enhancement factor over the simulation object (the field enhancement factor in the gap region) depends on resonance wavelength according to the variation of wing width, gap size, and thickness, and also the relationship between the geometry parameters and the resonance wavelength, are displayed in Fig.S6 to Fig.S8 as a supplement.

The optical property of the parabola-like gold nano-bowtie is quite sensitive to the polarization angle of the incident light wave. The enhancement factor in gap region depends on incident wavelength at various polarization angle is displayed in Fig.S9. It is obvious that the field enhancement factor in the gap region decreases with deviation of the polarization angle from 90 deg.

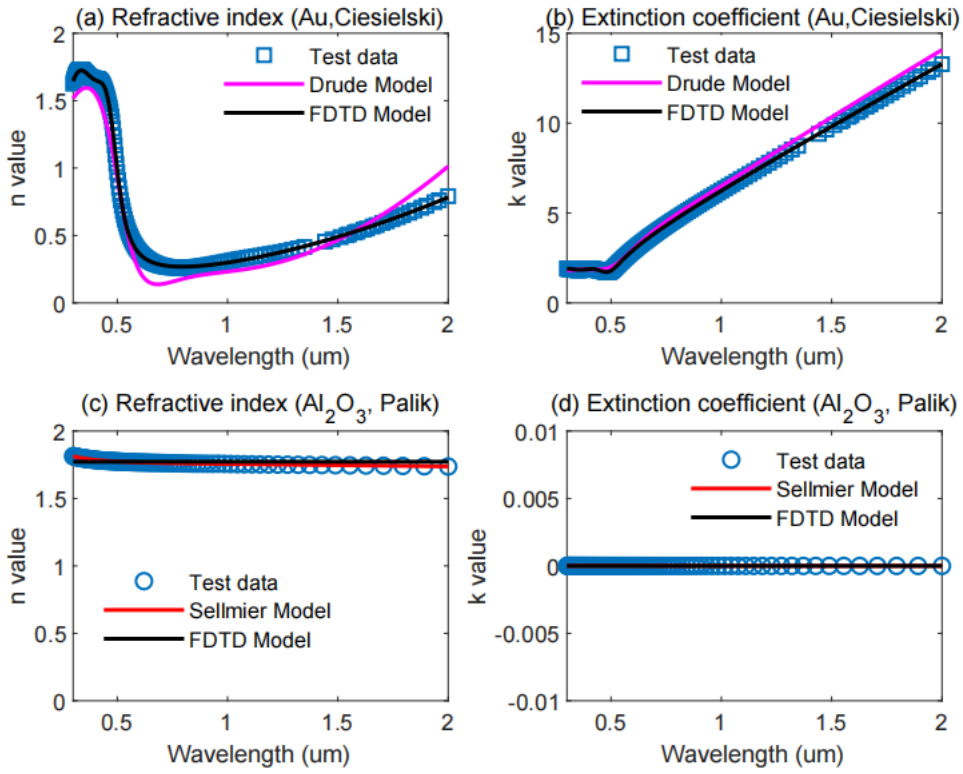

Figure S1. The refractive index of the gold material [4] [3] and sapphire used in the simulation [5]. (a) The test data of the refractive index of gold from ref [4] (blue square), the Drude model fitting of the test data with parameters from ref [2] (magenta line), and the FDTD model fitting with a RMS error less than 0.1 (black line). (b) The test data of the extinction coefficient of gold from ref [4] (blue square), the Drude model fitting of the test data with parameters from ref [2] (magenta line), and the FDTD model fitting with a RMS error less than 0.1 (black line). (c) The test data of the refractive index of sapphire from ref [5] (blue circle), the Sellmier model fitting of the test data with parameters from ref [3] (red line), and the FDTD model fitting with a RMS error less than 0.1 (black line). (d) The test data of the extinction coefficient of sapphire from ref [5] (blue circle), the Sellmier model fitting of the test data with parameters from ref [3] (red line), and the FDTD model fitting with a RMS error less than 0.1 (black line).

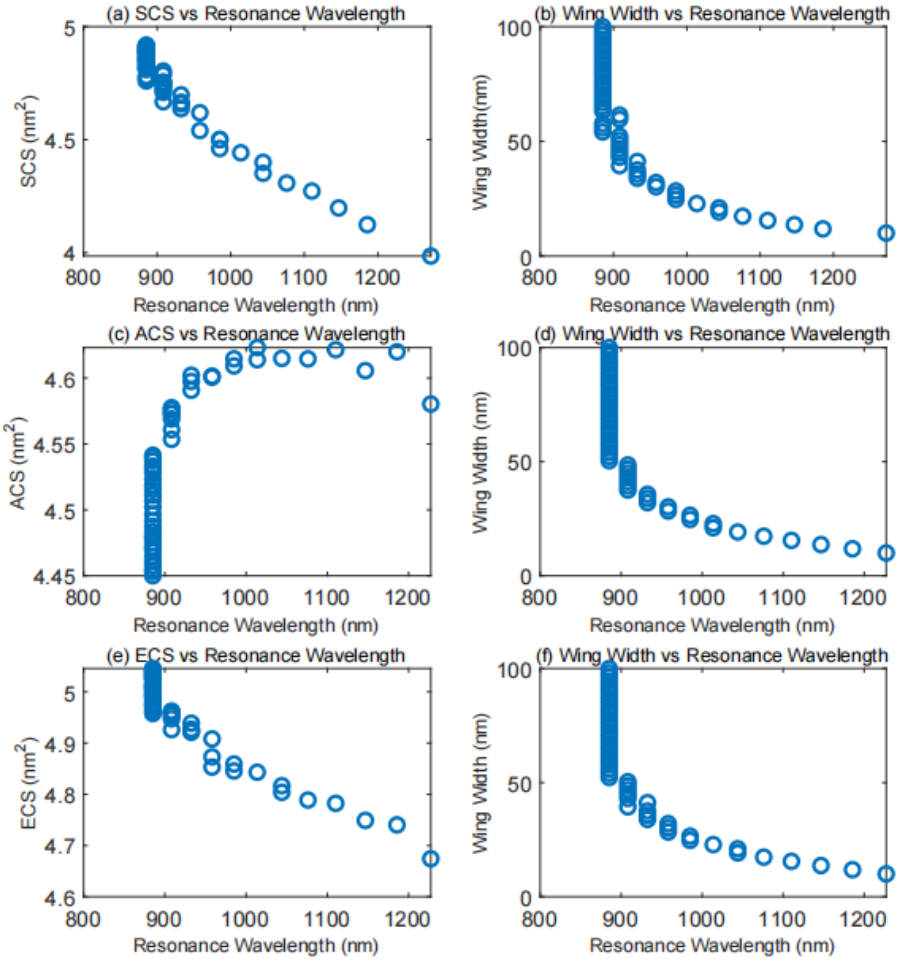

Figure S2. Various cross section dependent on resonance wavelength related with corresponding wing width. The values of the cross sections are in log scale. (a)~(b): scattering cross section dependent on resonance wavelength related with corresponding wing width. (c)~(d): absorption cross section dependent on resonance wavelength related with corresponding wing width. (e)~(f): Extinction cross section dependent on resonance wavelength related with corresponding wing width.

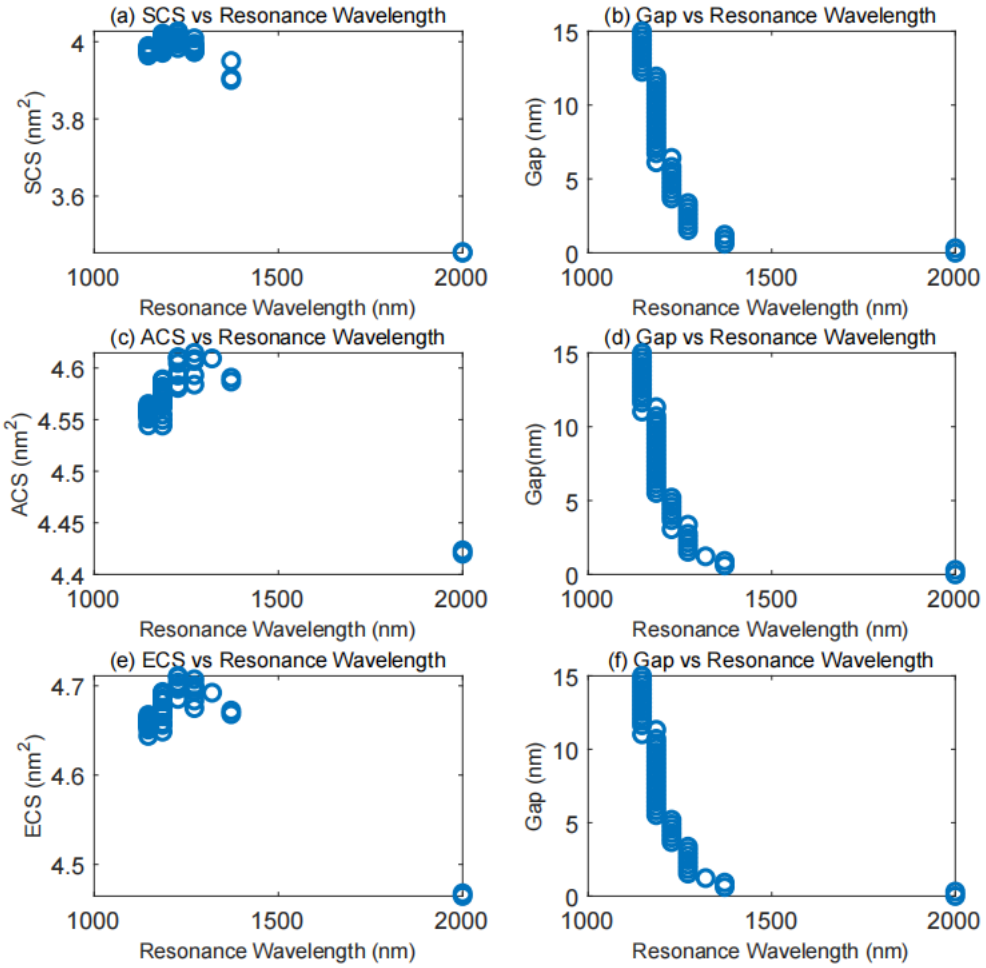

Figure S3. Various cross section dependent on resonance wavelength related with corresponding gap size. The values of the cross sections are in log scale. (a)~(b): scattering cross section dependent on resonance wavelength related with corresponding gap size. (c)~(d): absorption cross section dependent on resonance wavelength related with corresponding gap size. (e)~(f): Extinction cross section dependent on resonance wavelength related with corresponding gap size.

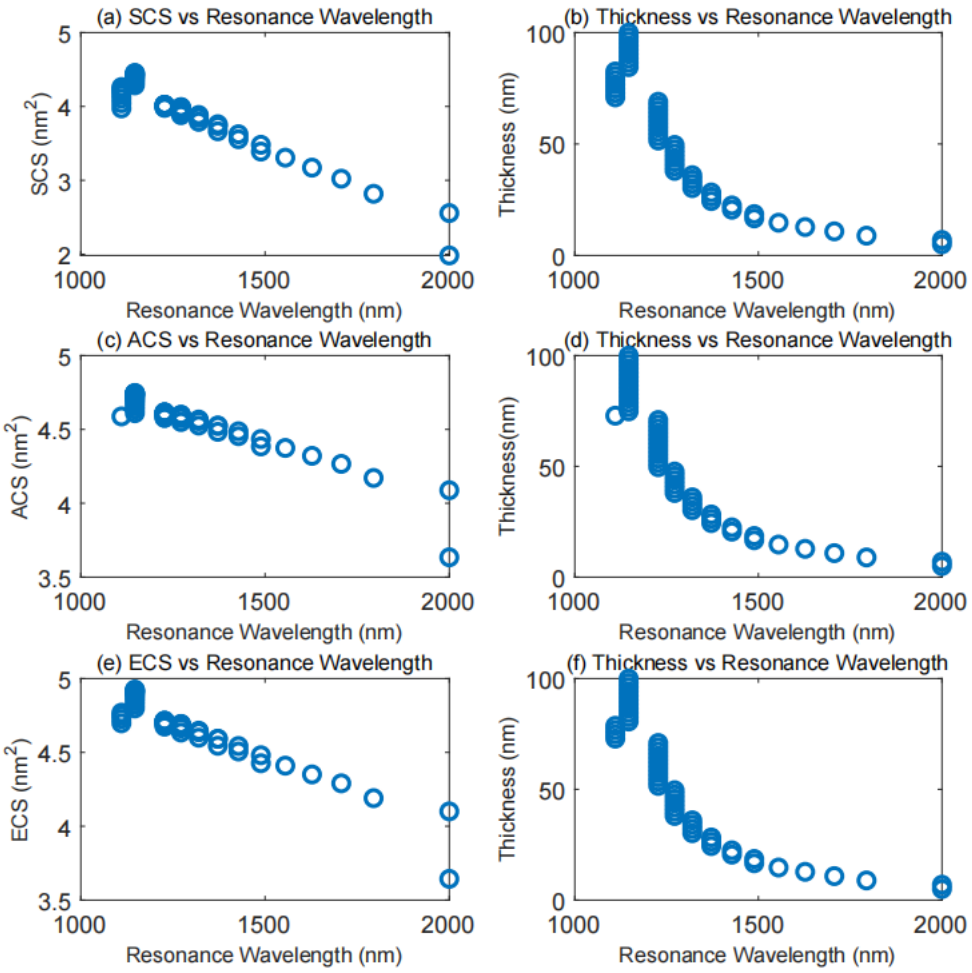

Figure S4. Various cross section dependent on resonance wavelength related with corresponding thickness. The values of the cross sections are in log scale. (a)~(b): scattering cross section dependent on resonance wavelength related with corresponding thickness. (c)~(d): absorption cross section dependent on resonance wavelength related with corresponding thickness. (e)~(f): Extinction cross section dependent on resonance wavelength related with corresponding thickness.

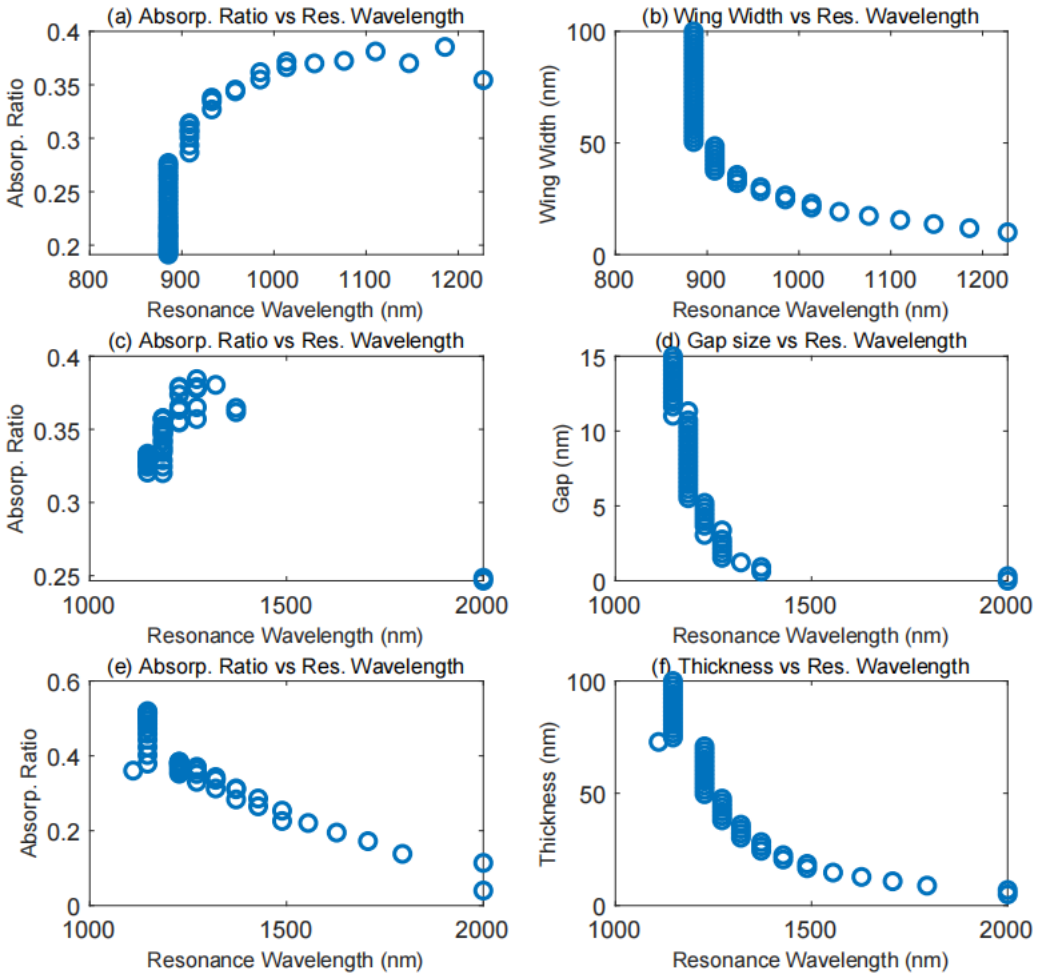

Figure S5. Absorption ratio dependent on resonance wavelength related with corresponding wing width, gap size, and thickness respectively. (a)~(b): Absorption ratio dependent on resonance wavelength related with corresponding wing width. (c)~(d): Absorption ratio dependent on resonance wavelength related with corresponding gap size. (e)~(f): Absorption ratio dependent on resonance wavelength related with corresponding thickness.

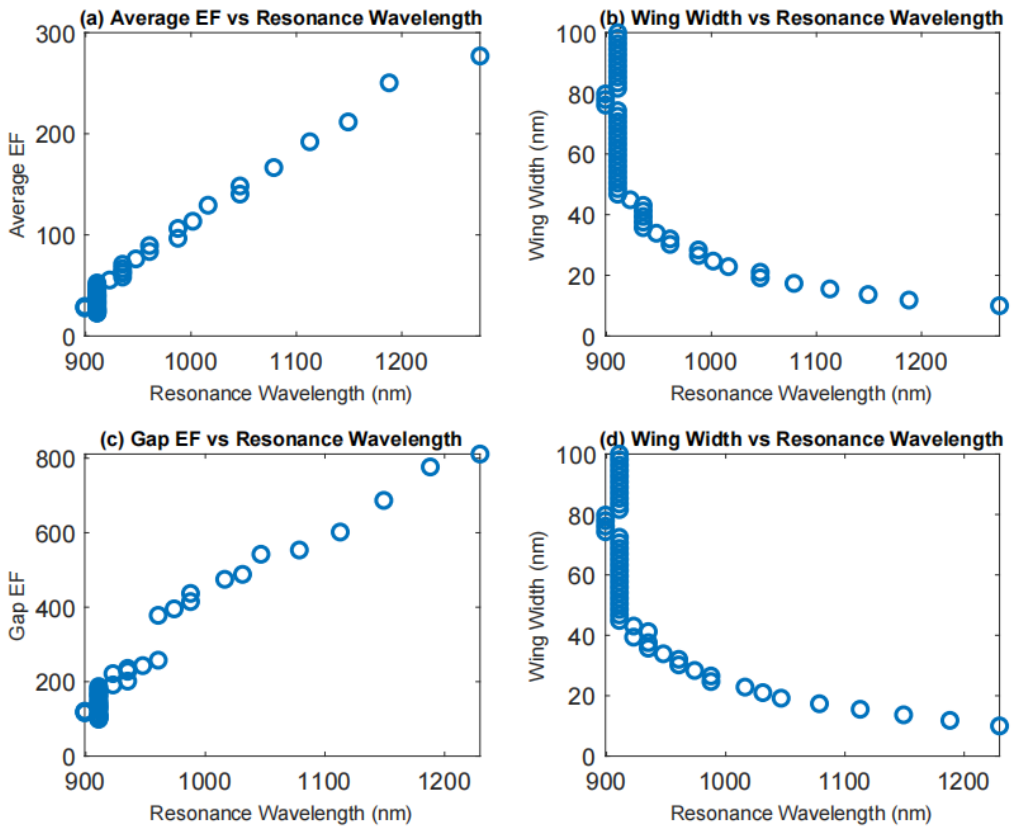

Figure S6. Average field enhancement factor over the simulation object and gap field enhancement factor in the gap region dependent on resonance wavelength related with corresponding wing width respectively. (a)~(b): Average field enhancement factor over the simulation object dependent on resonance wavelength related with corresponding wing width. (c)~(d): Average field enhancement factor over the gap region dependent on resonance wavelength related with corresponding wing width.

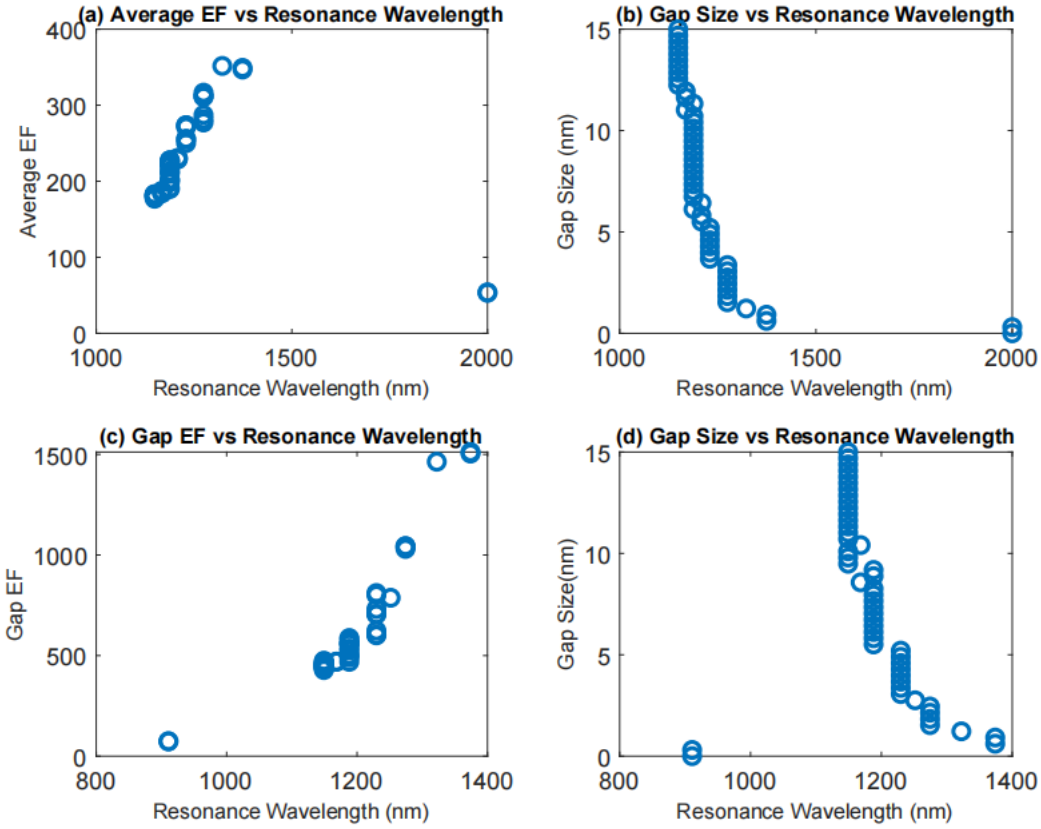

Figure S7. Average field enhancement factor over the simulation object and field enhancement factor in the gap region dependent on resonance wavelength related with corresponding gap size respectively. (a)~(b): Average field enhancement factor over the simulation object dependent on resonance wavelength related with corresponding gap size. (c)~(d): Average field enhancement factor over the gap region dependent on resonance wavelength related with corresponding gap size.

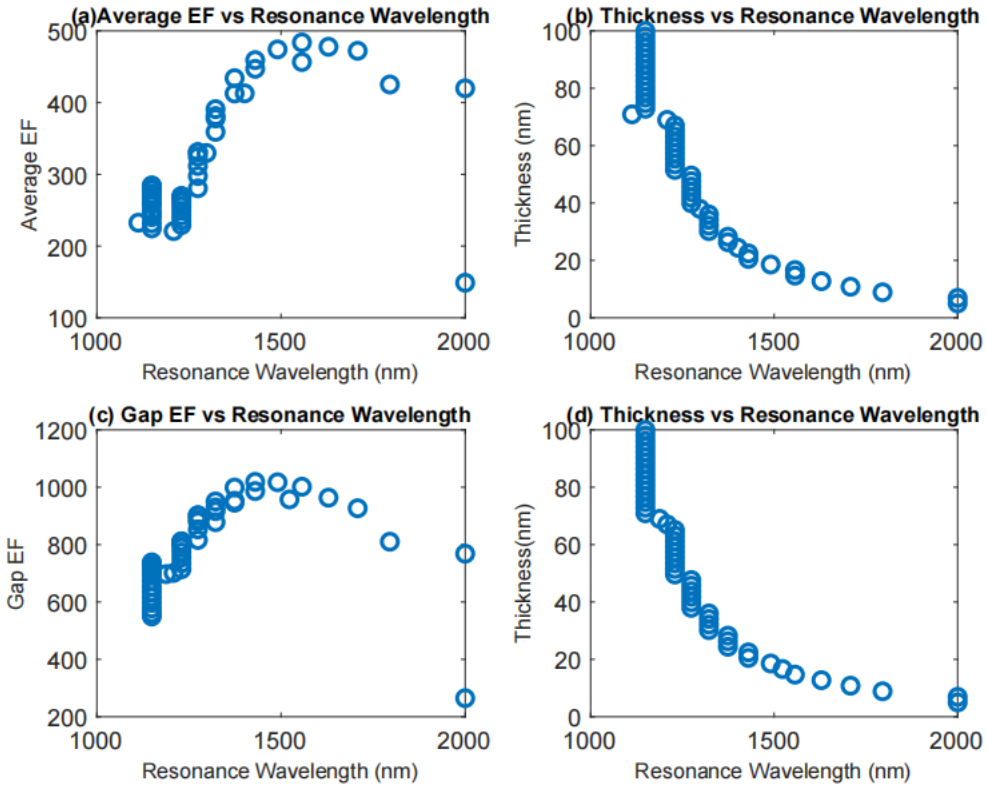

Figure S8. Average field enhancement factor over the simulation object and field enhancement factor over the gap region dependent on resonance wavelength related with corresponding thickness respectively. (a)~(b): Average field enhancement factor over the simulation object dependent on resonance wavelength related with corresponding thickness. (c)~(d): Average field enhancement factor over the gap region dependent on resonance wavelength related with corresponding thickness.

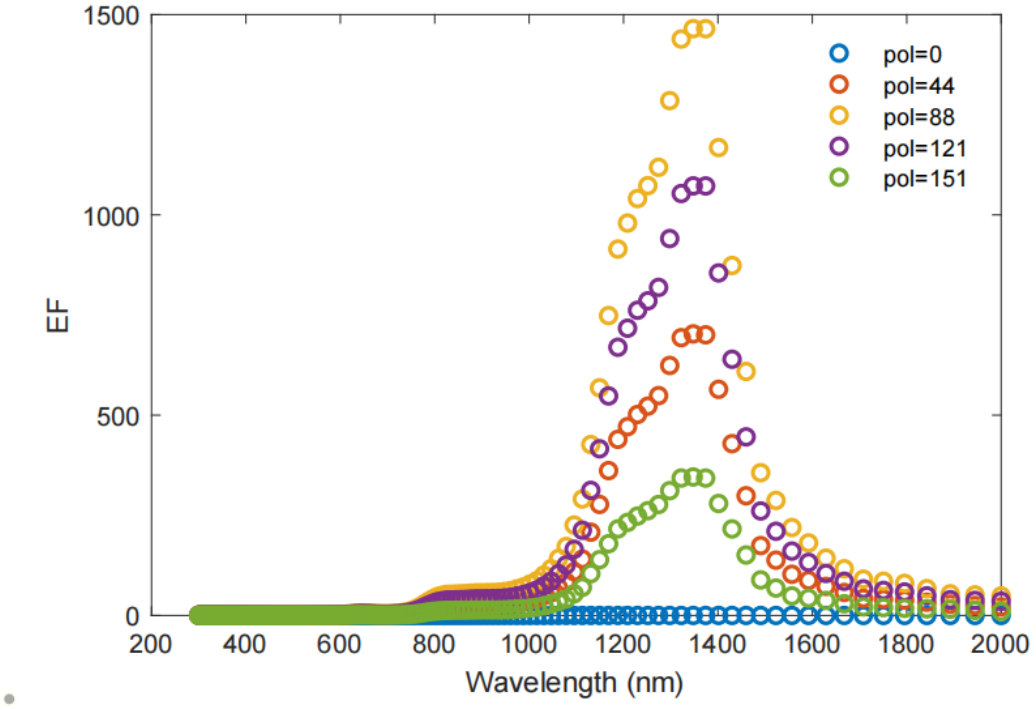

Figure S9. Average field enhancement factor over the gap region dependent on wavelength of the incident source at various polarization angle.

References

1. Maier, S., *Plasmonics: fundamentals and applications*. 2007, New York: Springer+Business Media LLC.
2. Hao, F. and P. Nordlander, *Efficient dielectric function for FDTD simulation of the optical properties of silver and gold nanoparticles.* Chemical Physics Letters, 2007. **446**(1): p. 115-118.
3. M. N. Polyanskiy, *Refractive index database*. https://refractiveindex.info.
4. Ciesielski, A., et al., *Evidence of germanium segregation in gold thin films.* Surface Science, 2018. **674**: p. 73-78.
5. Palik, E.D., *Handbook of optical constants of solids*. 1997, Maryland, US: Academic Press.
6. Hiroyuki Fujiwara, R.W.C., *Spectroscopic Ellipsometry for Photovoltaics*. 2018, Cham, Switzerland: Springer International Publishing AG.